

## The Structure of Aurichalcite, $(\text{Cu,Zn})_5(\text{OH})_6(\text{CO}_3)_2$ , Determined from a Microcrystal

BY MARJORIE M. HARDING AND B. M. KARIUKI

*Department of Chemistry, University of Liverpool, PO Box 147, Liverpool L69 3BX, England*

R. CERNIK

*DRAL Daresbury Laboratory, Warrington WA4 4AD, England*

AND G. CRESSEY

*The Natural History Museum, Cromwell Road, London SW7 5BD, England*

(Received 10 January 1994; accepted 28 June 1994)

### Abstract

Aurichalcite occurs as a natural mineral and also as a synthetically produced intermediate in the preparation of important copper/zinc oxide catalysts for a variety of industrial hydrogenation processes. Synchrotron radiation has allowed structure determination by single-crystal methods using a flake of material 5  $\mu\text{m}$  thick. The crystals are monoclinic and twinned. As in the related mineral hydrozincite,  $\text{Zn}_5(\text{OH})_6(\text{CO}_3)_2$  [Ghose (1964). *Acta Cryst.* **17**, 1051–1057], there are double layers of close-packed O atoms, with metal atoms in octahedral holes, as well as tetrahedrally coordinated metal atoms. In contrast to hydrozincite, there are also five-coordinate metal atoms. Alternate layers are linked only by hydrogen bonds and the metal coordination octahedra show strong tetragonal distortion. The tetrahedral sites are probably occupied by zinc, the other sites by zinc and copper.

### Introduction

Aurichalcite occurs naturally as a mineral. It is commonly found with malachite in the oxidized zones of zinc and copper deposits at Tomsk in Siberia, Santander in Spain, and Bisbee in Arizona; as a weathered product of zinc ores it is a useful guide to zinc deposits. It is also important as a synthetically produced intermediate in the preparation of copper/zinc oxide catalysts for a variety of industrial hydrogenation processes, for example in the production of methanol (Waller, Stirling, Stone & Spencer, 1989; Joyner, King, Thomas & Roberts, 1991; Pollard *et al.*, 1992). Despite the importance of knowledge of the structure for the understanding of its catalytic properties (Couves *et al.*, 1992), its crystal structure has remained unknown for many years. Early powder diffraction data (Jambor & Pouliot, 1965) allowed the determination of a unit cell, but not the structure; later attempts to determine the structure using synchrotron radiation powder diffraction were frustrated by the presence of impurities in the sample. The single crystals

available are not of adequate size for conventional X-ray structure analysis. Synchrotron radiation has now allowed diffraction data to be recorded from a minute flake of material and the structure has been determined by single-crystal methods. It is monoclinic and twinned, not orthorhombic as previously reported (Jambor & Pouliot, 1965).

Natural and synthetic aurichalcites are known with Cu/Zn ratios in the range 0.2–1 (Jambor & Pouliot, 1965; Couves *et al.*, 1992). The crystal used was selected from specimen BM1983,97 (Natural History Museum Collection), from Pima County, Arizona. The Cu/Zn atomic ratio was estimated, from edge-step heights in the X-ray absorption spectrum of the bulk sample, to be 0.67 (3):1.

### Experimental

Many details are given in Table 1. Data were recorded on the SRS wiggler beamline, workstation 9.6 (Helliwell *et al.*, 1986), at Daresbury Laboratory, with an Enraf–Nonius FAST (electronic area detector) diffractometer,  $0.4^\circ$  frames, exposure time 40 s per frame, covering  $200^\circ$  in  $\varphi$ , with the synchrotron ring current 20 mA (single bunch mode); processing of these images used *MADNES* software (Messerschmidt & Pflugrath, 1987) with local modifications for synchrotron radiation (Papiz, 1989).

From the symmetry of the intensities, and systematic absences, the unit cell appeared to be orthorhombic,  $B22_12$  or  $Bm2_1m$ , with  $a = 27.12(3)$ ,  $b = 6.419(1)$ ,  $c = 5.29(3)$  Å, in agreement with previous powder diffraction studies (Jambor & Pouliot, 1965). Attempts at structure solution by direct methods and Patterson methods in these and other orthorhombic space groups failed. The data set was expanded to four octants ( $hkl$ ,  $h\bar{k}l$ ,  $h\bar{k}\bar{l}$ ,  $hkl$ ) and interpretation of the Patterson in the space group  $B1$  (*i.e.* triclinic, no centre of symmetry, but  $B$  face-centred) was attempted. Five independent metal-atom positions were found quite easily (Zn or Cu, not distinguishable).

Table 1. *Crystal data, data collection and refinement parameters*

Crystal data	
Identification code	Aurichalcite
Empirical formula	(Cu,Zn) <sub>5</sub> C <sub>2</sub> H <sub>6</sub> O <sub>12</sub>
Formula weight*	545
Crystal system	Monoclinic
<i>a</i> (Å)	13.82 (2)
<i>b</i> (Å)	6.419 (3)
<i>c</i> (Å)	5.29 (3)
$\beta$ (°)	101.04 (2)
Space group	<i>P</i> 2 <sub>1</sub> / <i>m</i>
<i>V</i> (Å <sup>3</sup> )	461 (3)
<i>Z</i>	2
<i>D<sub>c</sub></i> (Mg m <sup>-3</sup> )	3.93
Wavelength (Å)	0.886 (5)
<i>F</i> (000)	524
$\theta$ range for cell parameters (°)	9.16–30.87
$\mu$ (mm <sup>-1</sup> )	22.7
Temperature (K)	293 (2)
Crystal size (mm)	0.1 × 0.04 × 0.005
Data collection	
Absorption correction	None
No. of measured reflections	1698
No. of independent reflections	410
No. of observed reflections	374
Observation criterion	$[I > 2\sigma(I)]$
<i>R</i> <sub>int</sub>	0.14
Range of <i>h, k, l</i>	−7 → <i>h</i> → 14 −7 → <i>k</i> → 7 −4 → <i>l</i> → 5
Refinement	
Refinement on	<i>F</i> <sup>2</sup>
Method of refinement	Full-matrix least squares
No. of reflections used in refinement	408
No. of parameters used	67
Goodness-of-fit	0.437
( $\Delta/\sigma$ ) <sub>max</sub>	0.01
$\Delta\rho$ <sub>max</sub> (e Å <sup>-3</sup> )	1.4
$\Delta\rho$ <sub>min</sub> (e Å <sup>-3</sup> )	−1.3
Final <i>R</i> indices	<i>R</i> 1 = 0.061, <i>wR</i> 2 = 0.156
$[I > 2\sigma(I)]$	
<i>R</i> indices (all data)	<i>R</i> 1 = 0.066, <i>wR</i> 2 = 0.165

\* Assuming 2Cu + 3Zn in empirical formula.

The electron-density map phased on these atoms showed five more peaks, initially assigned as oxygen; attempted refinement showed that they were more electron dense than oxygen, equivalent to approximately half a metal atom, and some were unreasonably close to each other. Inspection of the pattern of metal sites of full and half occupancy showed that it could represent one pattern of five atoms, repeated by the symmetry 2<sub>1</sub>/*m* overlaid on an equivalent pattern reflected in the (100) plane. The full occupancy metal atoms represented coincidence of the metal sites in both members of the twin, and the half occupancy atoms the other sites. The pattern of metal sites was similar, but not identical, to that in hydrozincite (Ghose, 1964). Three sites, *M*(1), *M*(2) and *M*(4), are on mirror planes and there are two of each per cell; the other site, *M*(3), is in a general position, of which there are four per cell. Thus, the pattern of five atoms, similar to that in hydrozincite (Ghose, 1964), is present twice in the unit cell.

Structure refinement was straightforward, using *SHELXL92* (Sheldrick, 1992). The distinction between

copper and zinc from diffractometer data alone is not easy and may require better diffraction data than a crystal of this size can provide. Site occupancy refinement, holding Zn + Cu = 1, and assigning one isotropic atomic displacement parameter to all metal atoms, was attempted. This indicated that the fraction of copper in each of *M*(1), *M*(2) and *M*(4) is *ca* 0.5 (2), while in *M*(3) it is *ca* 0.0 (2), which corresponds to an overall Cu:Zn ratio of 0.7 (2). Subsequently, these site occupancies were assigned and fixed, and the refinement was completed allowing anisotropic displacement parameters for the metal atoms, but not for any other atoms. H atoms were not located. The largest peaks in the final difference-density map were near the metal-atom sites; an absorption correction would have been desirable, but by the time this was realized the requisite information (*e.g.*  $\varphi$ -scans) was not available. The two components of the twin are present in the proportions 0.550 and 0.450 (*e.s.d.* 0.008).

The powder diffraction pattern calculated for this structure is in general agreement with the observed powder diffraction pattern (Cernik & Bell, 1994), confirming that the flake of material is typical of the bulk sample, and not a small impurity phase.

The orthorhombic cell originally assigned (Jambor & Pouliot, 1965) has the same *b* and *c* as the monoclinic cell proposed here, but *a*<sub>ortho</sub> is 2*a*<sub>mono</sub> + *c*<sub>mono</sub>; the cell is *B* face-centred and appears orthorhombic because (i)  $\beta$  is accidentally very close to 90° and (ii) the diffraction pattern has symmetry close to *mmm* as a result of the twinning.

## Results and discussion

The structure is illustrated in Figs. 1 and 2; atom coordinates are given in Table 2 and interatomic distances and angles in Table 3. There are double layers of close-packed O atoms, parallel to (100); these include all the hydroxyl ions and one oxygen from each carbonate ion. Within the double layer, *M*(2) is in a tetragonally distorted octahedral site, with two long and four short metal–oxygen distances (see Table 3), typical of Jahn–Teller distortion in Cu<sup>II</sup>; *M*(1) is in the other octahedral site and shows a smaller range of metal–oxygen distances, 1.94 (3)–2.24 (2) Å, with the two shortest in the *trans* configuration; this could be consistent with the inverse Jahn–Teller distortion in Cu<sup>II</sup>, or with Zn<sup>II</sup>. *M*(3) and *M*(4) are on the ‘outside’ of the double layer of O atoms and on opposite sides of it; they have tetrahedral and trigonal bipyramidal coordination, respectively. A model in which the three sites *M*(1), *M*(2) and *M*(4) are each occupied by copper or zinc with equal probability, and the tetrahedral site *M*(3) is entirely zinc, fits the diffraction data marginally better than any other assignment of the sites; it is also consistent with the observed stereochemistry and the ratio of Cu/Zn in the

bulk sample. The C(1) carbonate ion is bidentate in its coordination to  $M(4)$  and its third oxygen is coordinated to  $M(4)$  in the neighbouring cell along  $c$  (see Fig. 1). One oxygen of the other carbonate ion is coordinated to  $M(3')$  (related by  $2_1$ ) in the neighbouring double layer. Thus, on one side adjacent double layers are held together by hydrogen bonds from carbonate oxygen to hydroxyl groups, while on the other side carbonate ions in adjacent double layers are shared and there is an electrostatic interaction (see Fig. 2). The structure is similar to that of hydrozincite (Ghose, 1964), but in hydrozincite there are twice as many tetrahedral Zn atoms and no trigonal bipyramidal ones; all layers interact electrostatically by the sharing of carbonate ions between Zn(3) ions – none of the interactions depend only on hydrogen bonds.

Further characterization of the Cu/Zn distribution will be difficult, but is important. Samples with different

Table 2. Atomic coordinates ( $\times 10^4$ ) and equivalent isotropic displacement parameters ( $\text{\AA}^2 \times 10^3$ )

$$U_{eq} = (1/3)\sum_i \sum_j U_{ij} a_i^* a_j^* a_i \cdot a_j$$

	$x$	$y$	$z$	$U_{eq}$
$M(1)^*$	2371 (3)	7500	9282 (12)	9 (2)
$M(2)^*$	2478 (2)	4972 (3)	4206 (7)	9 (1)
$M(3)^*$	1242 (3)	2500	8655 (11)	9 (2)
$M(4)^*$	3913 (3)	2500	8839 (12)	9 (2)
O(1)	3115 (16)	7500	2990 (54)	6 (5)
O(2)	3282 (12)	9827 (19)	7607 (42)	4 (3)
O(3)	1804 (17)	2500	5446 (54)	7 (5)
O(4)	1617 (14)	9 (24)	10711 (48)	12 (4)
C(1)	4449 (23)	2500	3653 (85)	0 (6)
O(11)	3515 (20)	2500	2981 (63)	18 (6)
O(12)	4863 (20)	2500	6091 (69)	40 (6)
O(13)	5009 (18)	2500	1964 (59)	11 (6)
C(2)	536 (24)	7500	5141 (80)	0 (7)
O(21)	1521 (18)	7500	5916 (54)	8 (5)
O(22)	183 (16)	7500	2737 (50)	7 (5)
O(23)	60 (20)	7500	6990 (93)	22 (6)

\*  $M(3)$  was assigned as Zn;  $M(1)$ ,  $M(2)$  and  $M(4)$  were assigned as 0.5 Zn + 0.5 Cu.

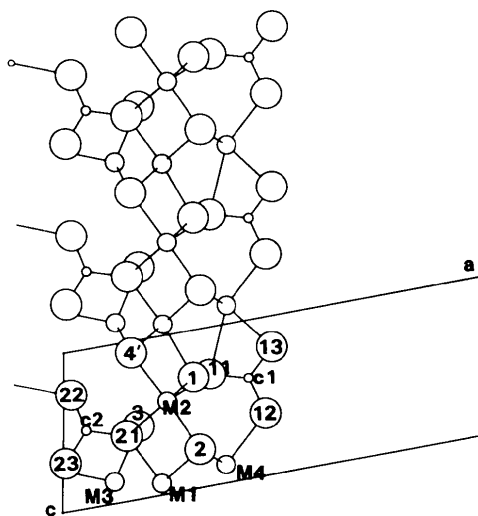


Fig. 1.  $b$ -axis projection of one layer in aurichalcite, showing the atom numbering. Oxygen atoms are indicated by number alone.  $O(4')$  is  $O(4)$  at  $x, y, z - 1$ . A line indicates the link of  $O(22)$  to  $M(3)$  of the neighbouring layer.

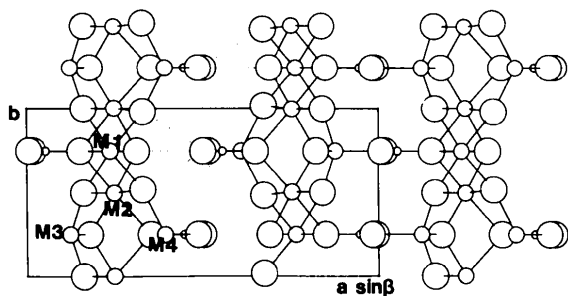


Fig. 2.  $c$ -axis view of aurichalcite structure, which shows how, at the boundary near  $x = 1/2$ , adjacent layers are linked by hydrogen bonds only (dotted lines), whereas at the boundary near  $x = 1$ , there are interactions between metal ions and O atoms of carbonate ions (full lines).

Table 3. Selected bond lengths ( $\text{\AA}$ ) and angles ( $^\circ$ )

$M(1)-O(21)$	1.94 (3)	$M(3)-O(3)$	2.00 (3)
$M(1)-O(1^i)$	2.03 (3)	$M(4)-O(2^{viii})$	1.978 (14)
$M(1)-O(4^{iiiii})$	2.13 (2)	$M(4)-O(13^i)$	2.02 (3)
$M(1)-O(2^{ivv})$	2.24 (2)	$M(4)-O(12)$	2.14 (3)
$M(1)-M(2^i)$	3.048 (14)	$M(4)-O(11^i)$	2.36 (4)
$M(2)-O(2^v)$	1.93 (2)	$C(1)-O(11)$	1.27 (4)
$M(2)-O(4^{vi})$	2.00 (2)	$C(1)-O(13)$	1.29 (5)
$M(2)-O(1)$	2.01 (2)	$C(1)-O(12)$	1.31 (6)
$M(2)-O(3)$	2.01 (2)	$C(2)-O(22)$	1.27 (5)
$M(2)-O(11)$	2.31 (2)	$C(2)-O(23)$	1.28 (6)
$M(2)-O(21)$	2.38 (2)	$C(2)-O(21)$	1.34 (4)
$M(3)-O(4^{iiiv})$	1.95 (2)	$O(4^{ii})-M(3)-O(22^{vii})$	110.4 (7)
$M(3)-O(22^{vii})$	1.97 (2)	$O(4)-M(3)-O(3)$	111.7 (8)
$O(21)-M(1)-O(1^i)$	173.2 (10)	$O(22^{vii})-M(3)-O(3)$	101.9 (11)
$O(4^{iii})-M(1)-O(2^v)$	172.7 (6)	$O(2^{viii})-M(4)-O(2^v)$	120.4 (11)
$O(2^v)-M(2)-O(4^{vi})$	175.6 (7)	$O(2^{viii})-M(4)-O(13^i)$	119.0 (6)
$O(1)-M(2)-O(3)$	178.1 (8)	$O(13^i)-M(4)-O(11^i)$	60.7 (11)
$O(11)-M(2)-O(21)$	173.8 (11)	$O(12)-M(4)-O(11^i)$	156.2 (10)
$O(4^{ii})-M(3)-O(4)$	110.4 (13)		

$O-M-O$  angles between  $80$  and  $100^\circ$  are omitted.

$O \cdots O$  distances assigned as hydrogen bonds

$O(1) \cdots O(12^{iv})$	2.74 (5)	$O(3) \cdots O(23^{vii})$	2.66 (5)
$O(2) \cdots O(13^{iv})$	2.77 (5)	$O(4) \cdots O(22^v)$	2.91 (5)

Symmetry codes: (i)  $x, y, z + 1$ ; (ii)  $x, -y + \frac{1}{2}, z$ ; (iii)  $x, y + 1, z$ ; (iv)  $x, y, z$ ; (v)  $x, -y + \frac{3}{2}, z$ ; (vi)  $x, -y + \frac{1}{2}, z - 1$ ; (vii)  $-x, -y + 1, -z + 1$ ; (viii)  $x, y - 1, z$ ; (ix)  $-x + 1, -y + 1, -z + 1$ ; (x)  $x, y - 1, z + 1$ .

(bulk) Cu:Zn ratios and a number of single crystals from each must be studied. Synchrotron radiation with a wavelength close to the zinc or copper absorption edge would be most effective: at  $1.38 \text{\AA}$ , the real parts of the Cu and Zn scattering factors have the greatest difference; for Cu,  $f + f' = 27.6$  electrons, for Zn,  $f + f' = 21.7$  electrons [calculated with the program *FPRIME* (Cromer & Lieberman, 1970)].

The crystals are very thin flakes with perfect  $\{100\}$  cleavage, as might be expected of a layer structure held together by hydrogen bonds. The crystal quality is poor, giving very elongated diffraction spots and a

mosaic spread evaluated [in *MADNES*; Messerschmidt & Pflugrath (1987)] as 3.4°. Both the large mosaic spread and the twinning may be associated with the variable Cu:Zn composition, and a simple explanation can be suggested: a region rich in zinc, with little or no copper, should have a structure like hydrozincite, *i.e.* with tetrahedral *M*(3) on both sides of the oxygen double layer, whereas a copper content above a certain threshold presumably introduces distortions and leads to regions of aurichalcite structure with tetrahedral *M*(3) and trigonal bipyramidal *M*(4) on opposite sides of the double layer. The occasional insertion of the hydrozincite type of layer in the aurichalcite structure would lead to the observed twinning.

We are grateful to SERC for financial support and for the provision of synchrotron radiation facilities.

*Acta Cryst.* (1994). **B50**, 676–684

## Crystal Structure of the Commensurately Modulated $\zeta$ Phase of PAMC

BY P. HARRIS, F. K. LARSEN,\* B. LEBECH AND N. ACHIWA†

*Department of Solid State Physics, Risø National Laboratory, DK-4000 Roskilde, Denmark*

(Received 31 December 1993; accepted 28 March 1994)

### Abstract

The commensurately modulated  $\zeta$  low-temperature phase of bis(propylammonium) tetrachloromanganate(II), [NH<sub>3</sub>(C<sub>3</sub>H<sub>7</sub>)<sub>2</sub>]<sub>2</sub>MnCl<sub>4</sub>, has been determined at 8 K.  $a = 7.437$  (5),  $b = 7.082$  (5),  $c = 13.096$  (8) Å,  $\alpha = 105.59$  (1)°. Superspace group  $P2_1/b(0\beta 0)\bar{1}S$ , with  $\beta = 1/3$ ,  $V = 664.4$ ,  $Z = 2$ ,  $D_x = 1.58$  g cm<sup>-3</sup>, Mo  $K\alpha$  radiation,  $\lambda = 0.71069$  Å,  $\mu = 17.99$  cm<sup>-1</sup>,  $F(000) = 326$ ,  $wR(F) = 0.064$  for 1444 main reflections and  $wR(F) = 0.089$  for 248 satellite reflections. The modulation vector flips and locks into a commensurate value compared with the  $\epsilon$  phase, indicating a 'lock-in' and phase shift between adjacent modulated layers. The modulation waves do not change much from the values of the  $\epsilon$  phase, which confirms the lock-in of the modulation vector; only some components of the modulations of the propylammonium chains appear to be significantly different, these chains appear to be responsible for the phase shift across the layers.

\* Department of Chemistry, Århus University, DK-8000 Århus C, Denmark.

† Department of Physics, Kyushu University, Higashi-ku, Fukuoka, Japan.

### References

- CERNIK, R. J. & BELL, A. (1994). *J. Appl. Cryst.* **27**. In preparation.  
 COUVES, J. W., THOMAS, J. M., WALLER, D., JONES, R. H., DENT, A. J., DERBYSHIRE, G. E. & GREAVES, G. N. (1992). *Nature*, **354**, 465–468.  
 CROMER, D. T. & LIEBERMAN, D. (1970). *J. Chem. Phys.* **53**, 1891–1898.  
 GHOSE, S. (1964). *Acta Cryst.* **17**, 1051–1057.  
 HELLIWELL, J. R., PAPIZ, M., GLOVER, I. D., HABASH, J., THOMPSON, A. W., MOORE, P. R., HARRIS, N., CROFT, D. & PANTOS, E. (1986). *Nucl. Instrum. Meth. Phys. Res. A*, **246**, 617–623.  
 JAMBOR, J. L. & POULIOT, G. (1965). *Can. Mineral.* **8**(3), 385–389.  
 JOYNER, R. W., KING, F., THOMAS, M. A. & ROBERTS, G. (1991). *Catal. Today*, **10**, 417–419.  
 MESSERSCHMIDT, A. & PFLUGRATH, J. W. (1987). *J. Appl. Cryst.* **20**, 306–315.  
 PAPIZ, M. Z. (1989). Personal communication.  
 POLLARD, A. M., SPENSER, M. S., THOMAS, R. G., WILLIAMS, P. A., HOLT, J. & JENNINGS, J. R. (1992). *Appl. Catal. A*, **86**, 1–11.  
 SHELDRICK, G. M. (1992). *SHELXL92. Program for the Refinement of Crystal Structures*. Univ. of Göttingen, Germany.  
 WALLER, D., STIRLING, D., STONE, F. S. & SPENCER, M. S. (1989). *Faraday Discuss. Chem. Soc.* **87**, 107–129.

### 1. Introduction

The layered perovskite PAMC, bis(propylammonium) tetrachloromanganate(II), belongs to a structural family of compounds of the general formula (C<sub>n</sub>H<sub>2n+1</sub>NH<sub>3</sub>)<sub>2</sub>MX<sub>4</sub>, with  $M = \text{Mn}^{2+}$ ,  $\text{Cd}^{2+}$ ,  $\text{Fe}^{2+}$ ,  $\text{Cu}^{2+}$ ,  $\text{Cr}^{2+}$ ,  $\text{Pd}^{2+}$  and  $X = \text{Cl}^-$ ,  $\text{Br}^-$ . All these compounds consist of (MX<sub>6</sub>) octahedra sandwiched between the alkylammonium chains (see Fig. 1 for a schematic structure). The compounds having  $n = 3$  are unique as they exhibit the largest sequence of phase transitions (Depmeier, Felsche & Wildermuth, 1977; Depmeier, 1979). PAMC is additionally a two-dimensional antiferromagnet with a weak ferromagnetic moment and has been extensively studied both because of its structural and its magnetic properties.

The phase transitions are due to a gradual selection and ordering of the possible hydrogen bondings between the NH<sub>3</sub><sup>+</sup> groups and the Cl<sup>-</sup> ions, followed by a reorientation of the propylammonium chains. The tendency of the methyl ends of the chains to form an energetically favourable hexagonally packed layer, along with the constraint imposed by a nearly quadratic arrangement of the Cl octahedra, creates a frustration leading to the introduction of several